Title

Functional genomic analysis of frataxin deficiency reveals tissue-specific alterations and identifies the PPARγ pathway as a therapeutic target in Friedreich's ataxia

Permalink

https://escholarship.org/uc/item/7j5998gm

Journal

Human Molecular Genetics, 18(13)

ISSN

0964-6906

Authors

Coppola, Giovanni

Marmolino, Daniele

Lu, Daning

et al.

Publication Date

2009-07-01

DOI

10.1093/hmg/ddp183

Peer reviewed

Functional genomic analysis of frataxin deficiency reveals tissue-specific alterations and identifies the PPARγ pathway as a therapeutic target in Friedreich's ataxia

Giovanni Coppola[1], Daniele Marmolino[2], Daning Lu[1], Qing Wang[1], Miriam Cnop[3,4], Myriam Rai[2], Fabio Acquaviva[5], Sergio Cocozza[5], Massimo Pandolfo[2,†] and Daniel H. Geschwind[1,*,†]

[1]Program in Neurogenetics, Department of Neurology, David Geffen School of Medicine, University of California at Los Angeles, CA 90095, USA, [2]Laboratoire de Neurologie Expérimentale, [3]Division of Endocrinology and [4]Laboratory of Experimental Medicine, Hôpital Erasme, Université Libre de Bruxelles (ULB), 1070 Brussels, Belgium and [5]Department of Cellular and Molecular Biology, University of Naples 'Federico II', IEOS CNR, Via Pansini 5, 80131 Naples, Italy

Friedreich's ataxia (FRDA), the most common inherited ataxia, is characterized by focal neurodegeneration, diabetes mellitus and life-threatening cardiomyopathy. Frataxin, which is significantly reduced in patients with this recessive disorder, is a mitochondrial iron-binding protein, but how its deficiency leads to neurodegeneration and metabolic derangements is not known. We performed microarray analysis of heart and skeletal muscle in a mouse model of frataxin deficiency, and found molecular evidence of increased lipogenesis in skeletal muscle, and alteration of fiber-type composition in heart, consistent with insulin resistance and cardiomyopathy, respectively. Since the peroxisome proliferator-activated receptor gamma (PPARγ) pathway is known to regulate both processes, we hypothesized that dysregulation of this pathway could play a key role in frataxin deficiency. We confirmed this by showing a coordinate dysregulation of the PPARγ coactivator *Pgc1a* and transcription factor *Srebp1* in cellular and animal models of frataxin deficiency, and in cells from FRDA patients, who have marked insulin resistance. Finally, we show that genetic modulation of the PPARγ pathway affects frataxin levels *in vitro*, supporting PPARγ as a novel therapeutic target in FRDA.

INTRODUCTION

Friedreich's Ataxia (FRDA, OMIM #229300) is an inherited autosomal recessive disorder characterized by progressive neurologic disability, cardiomyopathy and, in some patients, diabetes mellitus (1). FRDA is caused by partial deficiency of the mitochondrial protein frataxin (2). Though the function of frataxin is still partly controversial, there is general agreement that it is involved in cellular iron homeostasis and that its deficiency results in multiple enzyme deficits, mitochondrial dysfunction, and oxidative damage. Complete absence of frataxin is incompatible with life in higher organisms, as demonstrated by the embryonic lethality observed in systemic and conditional gene knock-out models (3–6).

Residual frataxin amounts vary between 5 and 35% of normal levels in FRDA patients, and are little more than 50% in heterozygous carriers, who show no sign of disease (2). A clear pattern of selective vulnerability to this partial loss of frataxin can be observed in FRDA. In the nervous system, neurodegeneration affects the large primary sensory neurons in the dorsal root ganglia and their axons in peripheral nerves and in the dorsal columns of the spinal cord, the spinocerebellar pathways, the dentate nucleus in the cerebellum, the

---

*To whom correspondence should be addressed. Tel: +1 3107946570; Fax: +1 3102672401; Email: dhg@ucla.edu
†These authors co-directed this work.

distal part of the corticospinal tract and, to a variable extent, the auditory and visual pathways. Cardiac involvement is present in most patients at the preclinical level, and 45–63% of FRDA patients have hypertrophic cardiomyopathy, which can cause premature death (7,8). Overt diabetes is present in 14–19% of FRDA patients, and glucose intolerance is seen in 24–40% (9–11). Skeletal muscle is only sub-clinically involved in FRDA, as a reduced ATP production can be detected with MR spectroscopy (12), but the causal metabolic pathways have not been identified.

Reducing frataxin expression in mice to levels similar to those observed in FRDA (KIKO mice) induced a biochemical CNS phenotype (13) but not clinical abnormalities (14). To study the selective vulnerability to frataxin deficiency in a model where no confounding non-specific or secondary degenerative changes are expected to occur, we have utilized frataxin-deficient mice to investigate gene expression profiles in the heart, a major target of FRDA pathology, and in skeletal muscle, only sub-clinically affected in the human disease. This unbiased genome-wide analysis, which we further extended to liver and cellular models, confirmed the hypothesis that frataxin deficiency causes tissue-specific changes in several metabolic pathways. Involvement of the peroxisome-proliferator activator receptor gamma (PPARγ)/PPARγ coactivator 1 alpha (Pgc1a) pathway in several cell types may serve as key regulator of FRDA pathogenesis, including enhanced risk of diabetes and cardiomyopathy.

RESULTS

Functional genomic analysis of frataxin deficient mice

We analyzed tissue from heart and skeletal muscle from four KIKO mice compared with control littermates. We used two array platforms (Agilent G4121A and Illumina Mouse RefSeq Expression arrays, see Materials and Methods), in order to increase our detection power. Unsupervised array clustering clearly separates the two tissues (Fig. 1A), confirming distinct expression profiles. Because cardiac involvement is most clinically evident, we expected more changes in the cardiac tissue than skeletal muscle. However, in KIKO mice versus WT littermates, we found more differentially expressed (DE) genes in skeletal muscle ($n = 321$) than in heart ($n = 174$) (Fig. 1B and C), suggesting a level of complexity in the tissue-specific response to frataxin deficiency that we had not anticipated. We observed a preponderance of downregulated genes in both tissues. This confirms previous reports in this (13) and other (15) FRDA models, and suggests that frataxin deficiency induces a prevalent downregulation of gene expression. Furthermore, we observed distinct expression patterns in each muscle type, consistent with distinct downstream effects of frataxin deficiency in these distinct tissues.

Three-hundred and twenty-one probes (corresponding to 308 unique gene names) were DE between KIKO and WT skeletal muscle. The most DE genes are reported in Supplementary Material, Table S1, and the complete gene list is reported in Supplementary Material, Table S2. The top Gene Ontology (GO) categories (Supplementary Material, Table S1; Fig. 1D) include lipid metabolism (overall upregulated), transcriptional regulation and signal transduction.

Ingenuity Pathway analysis (Supplementary Material, Fig. S1) showed that a number of targets of the transcriptional regulator *Srebp1* (including *Acas2*, *Scd2* and *Aacs*) were also upregulated in skeletal muscle. We also observed increased levels of *Socs3*, which has been linked to insulin resistance (16) and diabetes (17). Interestingly, we found a significant upregulation of the cytosolic malic enzyme 1 (*Mod1*), confirming a previous report of increased activity in FRDA muscle biopsies (18). Some contractile proteins were also dysregulated (mostly downregulated) in skeletal muscle, including *Tnn1*, *Myl3*, *Tnnc1*. We observed an over-representation of downregulated contractile proteins expressed in slow-twitch fibers, which would lead to a prevalence of fast, more anaerobic, less-oxidative fiber type, in contrast to the signature observed in cardiac muscle (see in what follows).

One-hundred and seventy-four probes (corresponding to 169 unique gene names) showed differential expression in heart (Supplementary Material, Tables S3 and S4). The top GO categories (Supplementary Material, Table S3; Fig. 1E) include 'regulation of muscle contraction' (overall downregulated), 'oxidoreductase activity' and 'regulation of cell cycle'. Ingenuity Pathway analysis (Supplementary Material, Fig. S2) showed an overrepresentation of mitogen-activated kinase (*Mapk*) targets, confirming the involvement of this pathway as an early biochemical change in response to frataxin deficiency (13). Most strikingly, in heart a number of core proteins of the muscle-fiber contractile apparatus showed significant downregulation, including *Myh4*, *Tnnc2* and *Tnni2* (Supplementary Material, Table S3). Downregulated genes were mostly associated with aerobic, fast-twitch myofibrils (e.g. *Atp2a1*, *Tnnc2*, *Tnni2*, *Tnnt3*)—an opposite trend compared with skeletal muscle. *Atp2a1* (also known as sarcoplasmic/endoplasmic reticulum calcium ATPase 1, *Serca1*) is involved in calcium sequestration and muscular excitation/contraction. Downregulation of SERCAs has been associated with cardiomyopathy in a number of studies (19), and its upregulation is beneficial for cardiac function in animal models (20). Only 6% of DE genes in heart were also dysregulated in skeletal muscle, indicating a differential effect of frataxin deficiency on these two metabolically distinct muscle tissues.

We selected 14 genes to represent a cross-section of DE genes expressed at different levels and in different tissues, for validation by qPCR. We confirmed ∼71% of the targets (Fig. 1F)—a high confirmation rate, considered the magnitude of the observed changes and the sensitivity of qPCR.

Taken together, these data suggest an upregulation of lipidogenic enzymes in skeletal muscle, and a shift in fiber-type composition in both heart and skeletal muscle, in opposing directions. In heart, these expression changes, together with changes in calcium-related genes (21), are compatible with early signs of cardiomyopathy, whereas in skeletal muscle (a major insulin target) these data suggest a derangement of fuel metabolism related to early changes occurring in insulin resistance and type 2 diabetes (T2D). Pgc1a and the sterol-responsive element binding protein 1 (Srebp1) are master regulators of lipid biosynthesis and breakdown (22,23). *Pgc1a* is also known to control the muscle fiber-type ratio (24), and both factors are involved in insulin resistance and diabetes (25–27). Since the dysregulation of these two master transcriptional regulators provides a parsimonious explanation
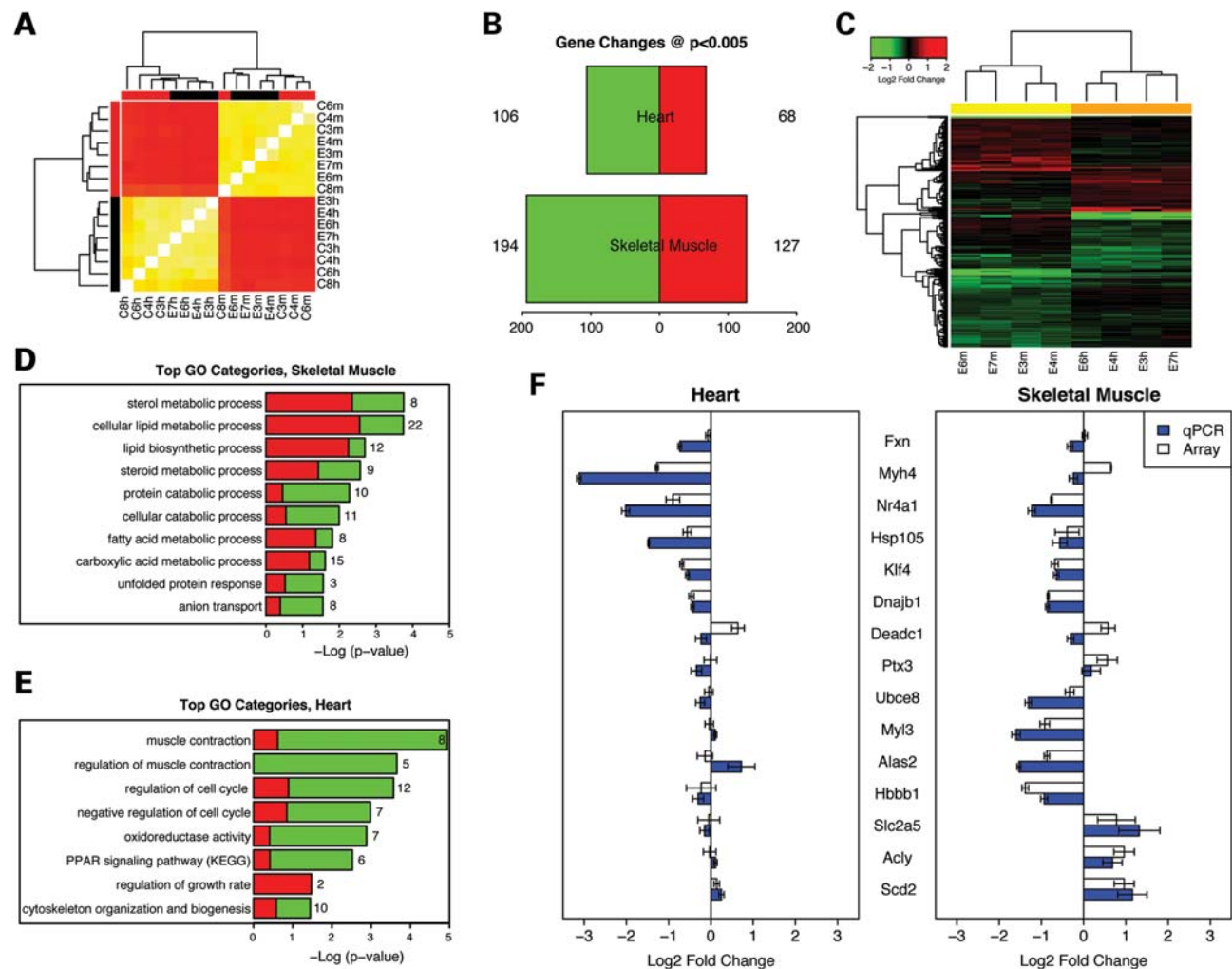
Figure 1. Microarray analysis of heart and skeletal muscle in KIKO mice. (**A**) Array clustering based on mean average deviation shows sample clustering by tissue. Within tissues, samples tend to cluster by genotype. Color coding bars: Top (genotype): red, WT samples; black, KIKO samples. Left side (tissue): red, skeletal muscle samples; black, heart samples. (**B**) Number of differentially expressed genes at $P < 0.005$. Three-hundred and twenty-one probes (194 down-regulated, 127 upregulated) were differentially expressed in skeletal muscle; 174 (106 downregulated, 68 upregulated) in heart of KIKO mice versus WT; (**C**) Heatmap depicting fold changes in cardiac and skeletal muscle samples in KIKO mice versus controls. Shades of red represent upregulation, shades of green downregulation. Genes and samples are clustered by similarity. Most genes have tissue-specific changes, whereas a subset of genes present changes across tissues. Color coding bar: yellow, skeletal muscle samples (KIKO versus average of WT); orange: heart samples (KIKO versus average of WT); (**D** and **E**) Gene ontology analysis of differentially expressed genes in heart and skeletal muscle samples from KIKO versus WT mice. Top categories include 'sterol' and 'lipid metabolic process' in skeletal muscle and 'regulation of muscle contraction' in heart. Bars represent the −Log of the over-representation *P*-value, as calculated by the DAVID algorithm (http://david.abcc.ncifcrf.gov/). Red and green represent the proportion of up and downregulated genes, respectively. The number at the end of the bar represents the number of probes differentially expressed in each category; (**F**) Real-time quantitative PCR (qPCR) confirmation on 14 among the top differentially expressed genes. Fold changes are expressed in log2. Error bars: standard error. qPCR confirmed tissue specificity (e.g. *Myh4* only downregulated in heart, *Scd2*, *Slc2a5*, *Acly* only upregulated in skeletal muscle).

for the tissue-specific transcriptional changes that we observed, we hypothesized that they are directly affected by frataxin deficiency. Further supporting this hypothesis, we found that other genes whose expression is affected by *Pgc1a* [e.g. *Mmp9* (28), *Fabp3* (29), *Socs3* (30)] are also dysregulated.

We generated cellular models of frataxin deficiency using short hairpin RNA interference (shRNAi) and followed the effects of transient frataxin downregulation on a set of target genes identified in the microarray study. In such models, expression changes occurring over a short time period (12–72 h) can be more confidently attributed to a direct, primary

effect of frataxin deficiency, rather than a secondary degenerative process due to long-term cellular changes.

Transfection of C2C12 myoblasts with an anti-frataxin shRNA (shRNAi^Fxn) induced an average 50% downregulation of the *Fxn* transcript and protein that started at 12 h, peaked at 24–32 and lasted up to 72 h (Fig. 2A and B). In these cells, we observed dysregulation of a set of genes already known to be downstream of frataxin deficiency, such as *Isu* (31) and *Mthf* (15), thus validating them as a cellular model of frataxin deficiency. Consistent with our interpretation of the microarray findings in KIKO skeletal muscle, we found a coordinate downregulation of *Pgc1a* and upregulation of *Srebp1*
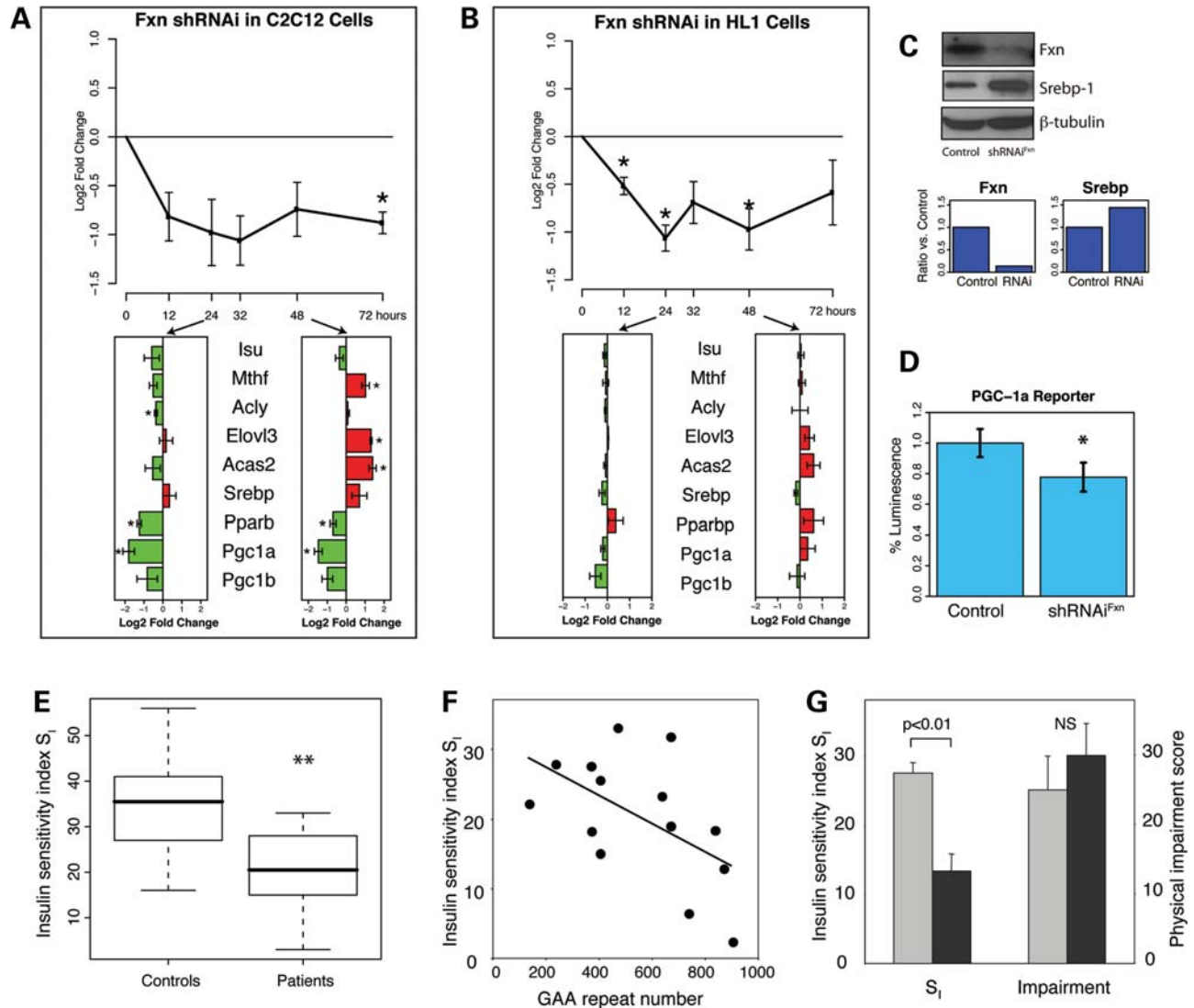
Figure 2. C2C12 (**A**) and HL-1 (**B**) cells were transfected with shRNAi for frataxin. Expression levels of frataxin versus cells transfected with control shRNAi were assessed at 12, 24, 32, 48 and 72 h after transfection (top panel). Expression levels of nine genes were assessed at 24 and 48 h after transfection (bottom panel). Red bars: upregulated genes; green bars: downregulated genes. Fold changes are expressed in log2. Error bars: standard error. Asterisk: $P < 0.05$, one-sample *t*-test. (**C**) Representative western blots (top) and blot quantification (bottom) for Frataxin and Srebp1 after transfection with control shRNAi (left) and shRNAi^{Fxn} (right). (**D**) shRNAi^{Fxn} transfection reduces Pgc1a expression as measured by a luciferase assay in 293 cells after 24 h. (**E**) FRDA patients have a significantly lower insulin sensitivity index: boxplots representing the insulin sensitivity index S_I [$\times 10^{-5}$ min^{-1}/(μU/ml)] in healthy controls and FRDA patients, matched for age and body mass index. $n = 14$ in each group, **$P < 0.005$ by Wilcoxon rank sum test. (**F**) In FRDA patients, S_I was significantly inversely correlated with the number of GAA repeats on the smaller FRDA allele ($r = -0.55$, $P < 0.05$). (**G**) Physical impairment scores are not significantly different between insulin-resistant and insulin-sensitive patients; the bar graph depicts the S_I (left) and the physical impairment scores [on a scale from 0 (normal) to 42 (most severe impairment), right] of the 50% ($n = 7$) most insulin sensitive (light gray bars) and of the 50% ($n = 7$) most insulin resistant patients (dark gray bars); $P = 0.5$ for comparison between the two groups.

(Fig. 2A,C,D). Accordingly, two out of three tested lipogenic genes that were upregulated in KIKO skeletal muscle (*Elovl3*, *Acas2*, *Acly*) also showed a significant upregulation in shRNAi^{Fxn}-transfected C2C12 cells, peaking at 48 h after transfection (24 h after frataxin downregulation, Fig. 2A). In addition, PPAR-binding protein (*Pparbp*), which was downregulated in brains of KIKO mice and fibroblasts from FRDA patients (13), was also downregulated.

To check the specificity for skeletal muscle-derived cells of the above changes, as suggested the by microarray data, we generated shRNA^{Fxn}-transfected HL-1 cardiomyocytes.

Though these cells showed a 40–50% frataxin mRNA downregulation, no significant changes in lipogenic genes occurred, whereas *Pparbp* and *Pgc1a* showed a non-significant trend towards upregulation (Fig. 2B), in concordance with the KIKO heart expression profiling findings.

We next tested the hypothesis that the changes observed in skeletal muscle represent systemic metabolic changes consistent with fuel shift and potential insulin resistance. Because liver is a major player in fuel metabolism and insulin response, we analyzed global patterns of gene expression in the liver of 3 KIKO mice compared to 3 WT mice using microarrays. This

analysis identified 182 DE probes in KIKO versus WT mice (Supplementary Material, Fig. S3 and Table S5). Strikingly, by GO analysis, lipid metabolism was among the top categories showing a significant enrichment in liver (Supplementary Material, Fig. S3B). Many dysregulated genes were shared with skeletal muscle (e.g. *Acac*, *Acas2*). In addition, other lipid-related genes showed liver-specific changes (Supplementary Material, Table S5), consistent with a systemic metabolic rearrangement towards increased lipogenesis in frataxin deficiency. These observations further suggest that *Pgc1a* and *Srebp1* are likely to play a central role in this transcriptional response. To summarize this concept, a potential model that is parsimonious with these data is depicted in Supplementary Material, Figure S4.

FRDA patients are insulin resistant

The finding that gene expression profiles in KIKO mice skeletal muscle and liver were suggestive of decreased insulin sensitivity prompted us to test insulin sensitivity in 14 non-diabetic FRDA patients by intravenous glucose-tolerance testing and minimal model analysis of glucose kinetics. Confirming previous reports (9,32), we found that non-diabetic FRDA patients were insulin resistant compared with controls [insulin sensitivity index S_I 20 ± 2 in patients versus $34 \pm 3 \times 10^{-5}$ min^{-1}/(μU/ml) in healthy controls matched for age and body mass index, $n = 14$ in each group, $P < 0.005$, Fig. 2E and G]. Furthermore, insulin sensitivity was significantly inversely correlated with the number of GAA repeats in the smaller FRDA allele ($r = -0.55$, $P < 0.05$, Fig. 2F) in FRDA patients, indicating that it is directly linked to the degree of frataxin deficiency. To exclude that the severity of neurological impairment, possibly because of the resulting reduced motor activity, rather than the degree of frataxin depletion was the cause of insulin resistance, we compared the score on a neurological impairment rating scale ranging from 0 (normal) to 42 (most severe impairment) between the 50% more insulin sensitive FRDA patients ($n = 7$) and the 50% more insulin resistant patients ($n = 7$), and found no significant difference (Fig. 2G), suggesting that frataxin deficiency directly causes insulin resistance, independent of physical impairment.

The PPARγ pathway is dysregulated in frataxin deficient mice and FRDA patients

We assessed whether *Pgc1a* is dysregulated in additional cell types, including CNS cells, strengthening the causal connection between frataxin and Pgc1a downregulation. We cultured neural precursor cells (NPCs) from the subventricular zone (SVZ) from homozygous $Fxn^{(GAA)230}$ (KIKI) mice (33), KIKO mice and WT littermates and quantified *Fxn* and *Pgc1a* transcript levels using RT–qPCR. *Pgc1a* transcript levels were decreased by $\sim$25% in KIKI- and by $\sim$70% in KIKO-derived NPCs (Fig. 3A).

To extend these observations to human patients, we studied lymphoblastoid cell lines and primary skin fibroblasts from FRDA patients. In both cell types we observed a 70–80% downregulation of *PGC1A* relative to normal controls (Fig. 3A). Furthermore, when we examined results from

FRDA fibroblasts, a strong correlation emerged between *PGC1A* and *FXN* expression, normalized to controls ($r^2 = 0.9$, $P < 0.001$, Fig. 3B).
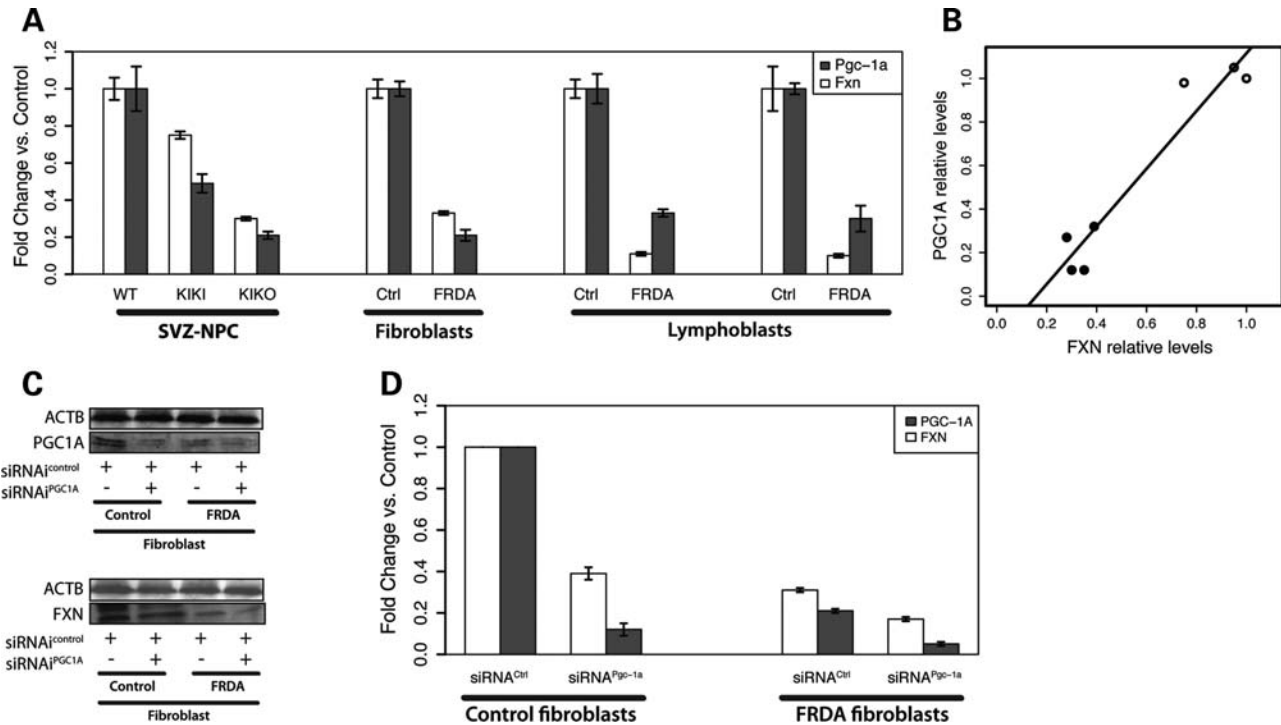
PPARγ manipulation affects frataxin levels

Pgc1a plays a key role in mitochondrial biogenesis and function by promoting the expression of several genes involved in mitochondrial DNA replication and in oxidative phosphorylation (34). The importance of frataxin for normal mitochondrial function makes it a possible target of PGC1A, prompting us to test whether PGC1A manipulation can affect frataxin levels. We downregulated PGC1A in human fibroblasts using a specific siRNA and observed a significant decrease in frataxin mRNA and protein levels after a 72-h transfection with siRNAi^{PGC1A} in both FRDA patients and controls (Fig. 3C and D). Thus, a positive feedback loop between PGC1A and frataxin levels appears to exist. We hypothesize that, when frataxin is primarily abnormally low, as in FRDA, the resulting impairment of this feedback loop is likely to further aggravate frataxin deficiency. Conversely, a pharmacological intervention to activate PGC1A should help re-establishing the positive feedback and therefore increase frataxin levels. The recent report that the potent PPARγ agonist Azelaoyl-PAF (35) is able to increase frataxin levels in FRDA cells (36) supports this model.

DISCUSSION

Neurodegenerative diseases affect specific subsets of neurons and in some cases non-nervous system structures as well, but the reasons underlying such selective cellular vulnerability are largely unknown. Reduced frataxin levels in FRDA are likely to have some downstream consequences that are the same in all cell types, along with consequences and adaptive responses that are cell and tissue-specific. We took an unbiased, genome-wide approach to obtain clues on FRDA pathogenesis and selective vulnerability. We analyzed how global gene expression profiles are affected in the heart (affected in FRDA), skeletal muscle and liver (not clinically affected) from a mouse model expressing frataxin at levels (about 30–35% of normal) corresponding to mildly affected FRDA patients, and yet not showing obvious clinical or pathological abnormalities. We observed the same basic pattern of dysregulation in skeletal muscle and liver, consistent with their roles in energy metabolism. However heart muscle, which is significantly affected by myopathy in the human disease, showed changes suggesting a fiber-type switch and dysregulation of contractile proteins, possibly consistent with cardiomyopathy.

Dysregulation of the PPARγ/PGC1A pathway was observed in tissues from animal and cellular models of frataxin deficiency, as well as in cells from FRDA patients, suggesting that this is a general downstream effector of frataxin deficiency. Pgc1a is the most studied of the peroxisome proliferator activated receptor co-activators (PGCs), a family of transcriptional co-activators that regulate mitochondrial biogenesis, energy substrate and utilization, and oxidative metabolism (23). In KIKO skeletal muscle and liver, our results

Figure 3. Genetic and pharmacologic modulation of the PPAR-γ pathway affects frataxin levels *in vitro*. (**A** and **B**) *Pgc1a* levels are correlated with frataxin levels in neural precursor cells from mouse models and in cells from patients with FRDA. (**A**) qPCR quantification of F*xn* (white bars) and *Pgc1a* (blue bars) in neural precursor cells from the subventricular zone (SVZ-NPC) in wild-type (WT, $n = 3$), KIKI ($n = 3$) and KIKO ($n = 3$) mice, and in lymphoblasts and fibroblasts from FRDA patients ($n = 4$) and normal controls ($n = 3$). KIKI mice express ~75% of normal frataxin levels, and KIKO ~30%. *Pgc1a* mRNA expression levels are reduced in all these cell lines, in a degree which is proportional to *Fxn* downregulation. Bars represent the average of six replicates, error bars represent the standard error. $P < 0.05$ for all the comparisons; (**B**) Relative *Pgc1a* levels are strongly correlated with relative *Fxn* mRNA levels ($r^2 = 0.9$, $P < 0.001$); qPCR quantification in fibroblasts from controls (open circles, $n = 3$) and FRDA patients (filled circles, $n = 4$). (**C** and **D**) *PGC1A* downregulation via siRNAi reduces frataxin protein levels in control fibroblasts, and further in FRDA fibroblasts. Western blotting analysis (**C**) and quantification (**D**) of PGC-1A (top) and FXN (bottom) protein 72 h after transfection with siRNAi[Pgc1a]. Control and FRDA are fibroblasts from healthy controls and patients, respectively. All experiments were performed on $n = 4$ FRDA cell lines and $n = 3$ control cell lines. Bars represent the average of six replicates, error bars represent the standard error. $P < 0.05$ for all comparisons.

indicate that *Pgc1a* activity is downregulated, as shown by the increased expression in both tissues of a set of genes involved in lipogenesis that are normally repressed by Pgc1a, including *Acas2*, *Scd2*, *Acly*, *Aacs*, *Elovl3*. These changes are also supported by the simultaneous upregulation of the transcription factor *Srebp1*. In skeletal muscle, changes in expression of contractile proteins that would result in increased glycolytic fast-twitch fibers and decreased slow, oxidative fibers type I and IIa, provide further evidence of downregulated Pgc1a activity (37). Pgc1a downregulation, and the related Srebp1 upregulation, are known to occur in insulin resistance and diabetes (38,39), along with reduced mitochondrial oxidative phosphorylation and lower oxidative-to-glycolytic muscle fiber ratio (40,41). The increased risk of diabetes in FRDA patients is therefore likely to be a consequence of the downregulation of *Pgc1a* in key tissues for insulin response and fuel metabolism control. FRDA patients are insulin resistant before being diabetic (9), and higher incidence of glucose intolerance and insulin resistance has been reported in family members of FRDA patients (42,43). However, other reports suggest a primary beta-cell involvement in FRDA (44), and a pathogenic mechanism primarily involving beta-cell failure has been proposed based on studies in other mitochondrial disorders (45,46) and on the pancreatic conditional frataxin

knock-out (6). Here, we confirm that insulin resistance is present in all tested non-diabetic FRDA patients, strongly supporting the hypothesis suggested by our gene expression data that insulin target tissues are relevant in the pathogenesis of diabetes in FRDA. Furthermore, we show here for the first time that the degree of insulin resistance of FRDA patients correlates with GAA repeat size (hence to lower residual frataxin levels) and is independent of neurological impairment, in agreement with the hypothesis that it is a direct consequence of frataxin deficiency.

Though the direct mechanistic link between frataxin and PGC1A remains to be completely defined, it is very likely related to mitochondrial dysfunction caused by frataxin deficiency. Mitochondrial dysfunction also occurs in T2D (47), as shown by 30% reduction of ATP production in skeletal muscle, associated with increased intramyocellular lipid (IML) content and decreased aerobic/anaerobic muscle fiber ratio (40,48). IML content, a consequence of increased lipid synthesis, is strongly correlated with glucose intolerance and insulin resistance in diabetic patients and can trigger insulin resistance (26). No data are available on IMLs in FRDA muscle, but the finding of increased cytosolic malic enzyme activity (18), in perfect concordance with gene expression data from KIKO mice, at least suggests increased lipogenesis
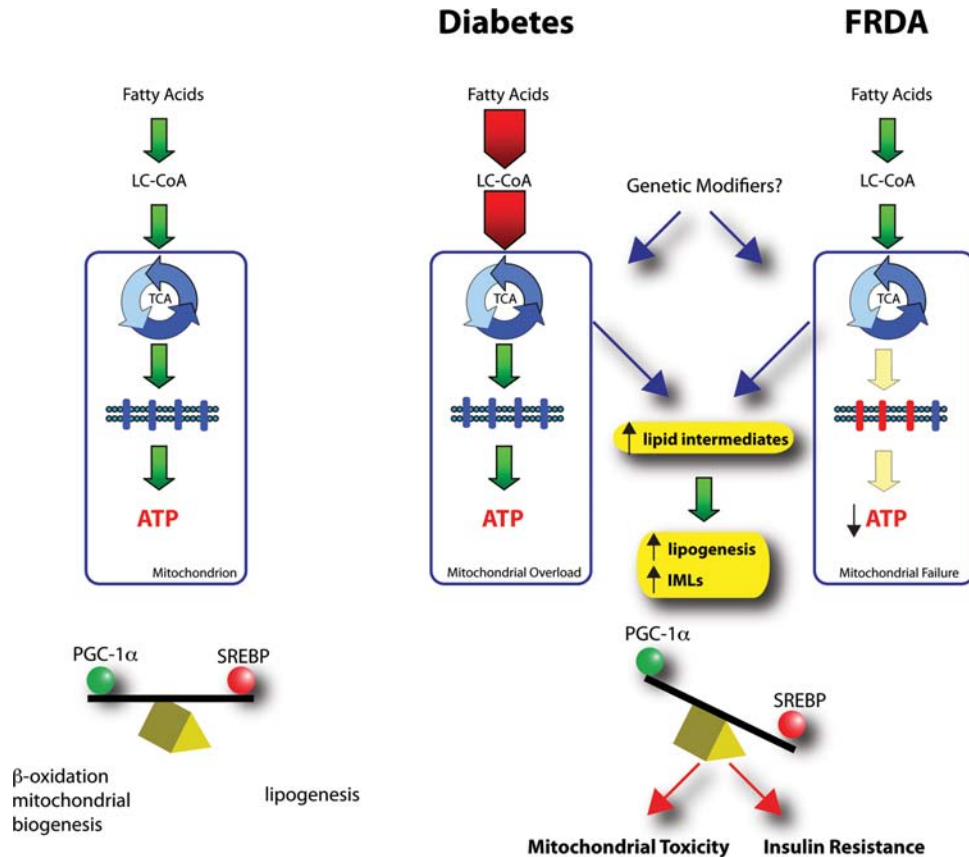
Figure 4. Diabetes in FRDA and type-2 diabetes may have a final common pathway. In normal conditions (left panel), lipid breakdown and biosynthesis are tightly controlled by the two master regulators *Pgc-1a* and *Srebp-1*. In type-2 diabetes (center), increased dietary lipids provided to the skeletal muscle can overload TCA and divert long-chain-CoA species into lipid precursors than can be converted in lipids, leading to an increased lipid intramyocellular content, which in turn leads to reduced glucose transport, reduced glycogen synthesis and ultimately to insulin resistance. In FRDA (right), deficits of TCA enzymes occur, as well as decreased activity of complexes I–II–III of the respiratory chain. An ineffective TCA and mitochondrial OXPHOS would lead to TCA overflow, favoring a metabolic shift toward the redirection of citrate from the TCA cycle and electron transport chain to processing into fatty acids. In mitochondrial diseases and in FRDA in particular, the oxidative stress can contribute to the diabetes pathogenesis at both (i) skeletal muscle and liver (insulin targets) and (ii) the beta-cell level, leading to overt diabetes mellitus. TCA, tricarboxylic acid cycle; IMLs, intra-myocellular lipids.

and a metabolic shift similar to T2D. We propose therefore that in FRDA, like in T2D, a state of insulin resistance and associated metabolic changes long precedes the onset of clinically overt diabetes, which is eventually due to pancreatic beta-cell failure. Beta-cell failure may in turn be accelerated by intrinsic mitochondrial dysfunction due to the gene defect (Fig. 4).

In contrast with skeletal muscle, we observed a downregulation of fast fibers in cardiac muscle, which also suggests an increased Pgc1a effect. We also observed a trend towards *Pgc1a* upregulation in HL-1 cardiomyocytes treated with shRNAi[Fxn]. Though apparently contradictory, these data actually confirm Pgc1a as a primary target of frataxin deficiency while underlining tissue-specific differences in this response. Our findings are indeed consistent with the observation that *Pgc1a* mRNA levels are elevated in the myocardium in a mouse model of metabolic syndrome (49) and with data suggesting a role for increased Pgc1a levels in diabetic cardiomyopathy (50). Furthermore, chronic overexpression of *Pgc1a* in hearts of transgenic mice induces cardiomyopathy (51,52), while only mild cardiac abnormalities are observed in the hearts of *Pgc1a* knock-out mice (53,54). The idea that Pgc1a

can have opposite changes in different tissues is supported by the fact that its overexpression induces uncoupled respiration in adipose tissue and coupling in cardiac myocytes (51). Pgc1a binding to tissue-specific transcription factors, enabling the activation of diverse metabolic programs in different tissues (23,55), offers an explanation for these differences and the distinct metabolic effects observed in skeletal and cardiac muscle in this model of frataxin deficiency (Supplementary Material, Fig. S4).

This model was supported by recent reports that (i) PGC1A overexpression in skeletal muscle cells (56) and (ii) treatment of FRDA cells with the PPARγ agonist Azelaoyl-PAF (36) are able to increase frataxin levels. PPARγ agonists such as rosiglitazone and pioglitazone are in clinical use as oral antidiabetics. The latter molecule may be of particular interest because of its capacity to cross the blood–brain barrier. Clearly, the opposite dysregulation of Pgc1a in the heart imposes caution for any attempt to clinically test such a drug in FRDA. Maybe not surprisingly, cardiac toxicity is a known side effect of this class of drugs.

In conclusion, we have identified distinct pattern of gene expression changes in metabolically distinct tissues in

a model of frataxin deficiency. These data suggest Pgc1a as a key regulator of gene expression that is directly affected by frataxin deficiency and in turn affects frataxin expression. Further studies (such as frataxin overexpression) are needed to characterize the relationship between Fxn and Pgc1a. Downregulation of Pgc1a is the rule in several frataxin-deficient cell types, including skeletal muscle, liver, lymphoblasts, fibroblasts and possibly the pathologically relevant CNS cells, engaging a feedback loop that leads to even lower frataxin levels, reduced antioxidant defenses and mitochondrial function. Such a mechanism appears to be responsible in particular for the vulnerability to diabetes of FRDA patients. In these cell types, upregulation of Pgc1a using PPARγ agonists may be an appealing therapeutic approach.

MATERIALS AND METHODS

Animals and tissue samples

Frataxin knockout/knockin (Frda$^{230GAA/-}$, KIKO) and knockin/knockin (Frda$^{230GAA/230GAA}$, KIKI) mice were obtained as described (14). Four 6-month-old male KIKO and three 6-month-old male KIKI mice were compared with age and gender-matched WT littermates. Total RNA from skeletal muscle (gastrocnemius), heart and liver was extracted by acid phenol extraction (Trizol, GIBCO/BRL) as recommended by the manufacturer.

Microarrays

Sample preparation and array hybridization and scanning were performed according to established protocols (detailed in Supplementary Material). Quality control, differential expression, and cross-platform microarray analysis were performed using Bioconductor packages in the R statistical environment (see Supplementary Material for a detailed description). The microarray data have been deposited in the NCBI Gene Expression Omnibus database (GEO, www.ncbi.nlm.nih.gov/geo) with the GEO series accession number GSE15849.

Cell culture

C2C12 cells were obtained from ATCC (Manassas, VA) and HL-1 cells were a kind gift from the Claycomb Lab (School of Medicine, LSU, New Orleans, LA). Fibroblasts primary cell cultures were obtained from skin biopsies of FRDA patients and healthy controls after receiving written informed consent. All the patients were homozygous for the GAA repeat expansion (500–1700 repeats), and were being treated with Idebenone 5 mg/kg. Epstein Barr virus-transformed lymphoblast cell lines GM15850 were from a FRDA patient (650–1030 GAA repeats; NIGMS, Human Genetic Cell Repository at the Coriell Institute, Camden, NJ, USA) and GM15851 from one unaffected control. Mouse neuronal precursor cells (NPC-SVZ) were obtained from wild-type and from KIKI/KIKO mice. Brain layer of tissue surrounding the ventricles was cultured in the media containing 20 ng/ml recombinant human EGF and 10 ng/ml recombinant human bFGF (Peprotech, NJ, USA). Derived neurospheres were plated in a fresh growth medium and were assessed for their character-

istics of self-renewal and multipotentiality. Cells were transfected using standard procedures, detailed in Supplementary Material.

qPCR experiments

Real-time quantitative PCR experiments were performed as described previously (13) and in Supplementary Material, Methods.

Western blot and luciferase assays

Western blot and luciferase assays were performed using standard procedures, detailed in Supplementary Material, Methods.

Assessment of physical impairment in FRDA patients

Speech, upright stability, upper limb coordination, and lower limb coordination scores from the FARS (57) scale were used.

Assessment of insulin sensitivity in FRDA patients and healthy controls

FRDA patients and healthy volunteers provided written informed consent. After an overnight fast, subjects underwent an intravenous glucose-tolerance test to measure insulin sensitivity. Glucose (0.3 g/kg) was infused intravenously, followed by an insulin infusion (0.025 U/kg) 20 min later, and blood was sampled at times -15, -5 and -1 min before intravenous glucose administration, and at 2, 3, 4, 5, 6, 8, 10, 14, 16, 19, 22, 23, 24, 25, 27, 30, 35, 40, 50, 60, 70, 80, 90, 100, 120, 140, 160 and 180 min (58). Plasma glucose was measured using the glucose oxidase method (DiaSys, Holzheim, Germany). Plasma insulin concentrations were measured by ELISA (INSI-CTK immunoradiometric analysis; DiaSorin, Saluggia, Italy). Insulin sensitivity was quantified as the insulin sensitivity index (S_I) based on the glucose and insulin data using the minimal model of glucose kinetics (59).

SUPPLEMENTARY MATERIAL

Supplementary Material is available at *HMG* online.

FUNDING

REFERENCES

1. Pandolfo, M. (2003) Friedreich ataxia. *Semin. Pediatr. Neurol.*, **10**, 163–172.
2. Campuzano, V., Montermini, L., Molto, M.D., Pianese, L., Cossee, M., Cavalcanti, F., Monros, E., Rodius, F., Duclos, F., Monticelli, A. *et al.* (1996) Friedreich's ataxia: autosomal recessive disease caused by an intronic GAA triplet repeat expansion. *Science*, **271**, 1423–1427.
3. Puccio, H., Simon, D., Cossee, M., Filipe, C., Tiziano, F., Melki, J., Hindelang, C., Matyas, R., Rustin, P. and Koenig, M. (2001) Mouse models for Friedreich ataxia exhibit cardiomyopathy, sensory nerve defect and Fe-S enzyme deficiency followed by intramitochondrial iron deposits. *Nat. Genet.*, **27**, 181–186.
4. Simon, D., Seznec, H., Gansmuller, A., Carelle, N., Weber, P., Metzger, D., Rustin, P., Koenig, M. and Puccio, H. (2004) Friedreich ataxia mouse models with progressive cerebellar and sensory ataxia reveal autophagic neurodegeneration in dorsal root ganglia. *J. Neurosci.*, **24**, 1987–1995.
5. Thierbach, R., Schulz, T.J., Isken, F., Voigt, A., Mietzner, B., Drewes, G., von Kleist-Retzow, J.C., Wiesner, R.J., Magnuson, M.A., Puccio, H. *et al.* (2005) Targeted disruption of hepatic frataxin expression causes impaired mitochondrial function, decreased life span and tumor growth in mice. *Hum. Mol. Genet.*, **14**, 3857–3864.
6. Ristow, M., Mulder, H., Pomplun, D., Schulz, T.J., Muller-Schmehl, K., Krause, A., Fex, M., Puccio, H., Muller, J., Isken, F. *et al.* (2003) Frataxin deficiency in pancreatic islets causes diabetes due to loss of beta cell mass. *J. Clin. Invest.*, **112**, 527–534.
7. Durr, A., Cossee, M., Agid, Y., Campuzano, V., Mignard, C., Penet, C., Mandel, J.L., Brice, A. and Koenig, M. (1996) Clinical and genetic abnormalities in patients with Friedreich's ataxia. *N. Engl. J. Med.*, **335**, 1169–1175.
8. Filla, A., De Michele, G., Coppola, G., Federico, A., Vita, G., Toscano, A., Uncini, A., Pisanelli, P., Barone, P., Scarano, V. *et al.* (2000) Accuracy of clinical diagnostic criteria for Friedreich's ataxia. *Mov. Disord.*, **15**, 1255–1258.
9. Finocchiaro, G., Baio, G., Micossi, P., Pozza, G. and di Donato, S. (1988) Glucose metabolism alterations in Friedreich's ataxia. *Neurology*, **38**, 1292–1296.
10. Shapcott, D., Melancon, S., Butterworth, R.F., Khoury, K., Collu, R., Breton, G., Geoffroy, G., Lemieux, B. and Barbeau, A. (1976) Glucose and insulin metabolism in Friedreich's ataxia. *Can. J. Neurol. Sci.*, **3**, 361–364.
11. Filla, A., DeMichele, G., Caruso, G., Marconi, R. and Campanella, G. (1990) Genetic data and natural history of Friedreich's disease: a study of 80 Italian patients. *J. Neurol.*, **237**, 345–351.
12. Lodi, R., Cooper, J.M., Bradley, J.L., Manners, D., Styles, P., Taylor, D.J. and Schapira, A.H. (1999) Deficit of in vivo mitochondrial ATP production in patients with Friedreich ataxia. *Proc. Natl Acad. Sci. USA*, **96**, 11492–11495.
13. Coppola, G., Choi, S.H., Santos, M.M., Miranda, C.J., Tentler, D., Wexler, E.M., Pandolfo, M. and Geschwind, D.H. (2006) Gene expression profiling in frataxin deficient mice: microarray evidence for significant expression changes without detectable neurodegeneration. *Neurobiol. Dis.*, **22**, 302–311.
14. Miranda, C.J., Santos, M.M., Ohshima, K., Smith, J., Li, L., Bunting, M., Cossee, M., Koenig, M., Sequeiros, J., Kaplan, J. *et al.* (2002) Frataxin knockin mouse. *FEBS Lett.*, **512**, 291–297.
15. Seznec, H., Simon, D., Bouton, C., Reutenauer, L., Hertzog, A., Golik, P., Procaccio, V., Patel, M., Drapier, J.C., Koenig, M. *et al.* (2005) Friedreich ataxia: the oxidative stress paradox. *Hum. Mol. Genet.*, **14**, 463–474.
16. Ueki, K., Kondo, T., Tseng, Y.H. and Kahn, C.R. (2004) Central role of suppressors of cytokine signaling proteins in hepatic steatosis, insulin resistance, and the metabolic syndrome in the mouse. *Proc. Natl Acad. Sci. USA*, **101**, 10422–10427.
17. Rieusset, J., Bouzakri, K., Chevillotte, E., Ricard, N., Jacquet, D., Bastard, J.P., Laville, M. and Vidal, H. (2004) Suppressor of cytokine signaling 3 expression and insulin resistance in skeletal muscle of obese and type 2 diabetic patients. *Diabetes*, **53**, 2232–2241.
18. Bottacchi, E. and Di Donato, S. (1983) Skeletal muscle NAD+(P) and NADP+-dependent malic enzyme in Friedreich's ataxia. *Neurology*, **33**, 712–716.
19. Inesi, G., Prasad, A.M. and Pilankatta, R. (2008) The Ca2+ ATPase of cardiac sarcoplasmic reticulum: Physiological role and relevance to diseases. *Biochem. Biophys. Res. Commun.*, **369**, 182–187.
20. Talukder, M.A., Kalyanasundaram, A., Zhao, X., Zuo, L., Bhupathy, P., Babu, G.J., Cardounel, A.J., Periasamy, M. and Zweier, J.L. (2007) Expression of SERCA isoform with faster Ca2+ transport properties improves postischemic cardiac function and Ca2+ handling and decreases myocardial infarction. *Am. J. Physiol. Heart Circ. Physiol.*, **293**, H2418–H2428.
21. Choi, K.M., Zhong, Y., Hoit, B.D., Grupp, I.L., Hahn, H., Dilly, K.W., Guatimosim, S., Lederer, W.J. and Matlib, M.A. (2002) Defective intracellular Ca(2+) signaling contributes to cardiomyopathy in Type 1 diabetic rats. *Am. J. Physiol. Heart Circ. Physiol.*, **283**, H1398–H1408.
22. Espenshade, P.J. and Hughes, A.L. (2007) Regulation of sterol synthesis in eukaryotes. *Annu. Rev. Genet.*, **41**, 401–427.
23. Finck, B.N. and Kelly, D.P. (2006) PGC-1 coactivators: inducible regulators of energy metabolism in health and disease. *J. Clin. Invest.*, **116**, 615–622.
24. Lin, J., Wu, H., Tarr, P., Zhang, C.-Y., Wu, Z., Boss, O., Michael, L., Puigserver, P., Isotani, E., Olson, E. *et al.* (2002) Transcriptional co-activator PGC-1[alpha] drives the formation of slow-twitch muscle fibres. *Nature*, **418**, 797–801.
25. Petersen, K., Dufour, S., Savage, D., Bilz, S., Solomon, G., Yonemitsu, S., Cline, G., Befroy, D., Zemany, L., Kahn, B. *et al.* (2007) The role of skeletal muscle insulin resistance in the pathogenesis of the metabolic syndrome. *PNAS*, 0705408104.
26. Petersen, K.F. and Shulman, G.I. (2006) Etiology of insulin resistance. *Am. J. Med.*, **119**(5 Suppl 1): S10–S16.
27. Savage, D.B., Petersen, K.F. and Shulman, G.I. (2007) Disordered lipid metabolism and the pathogenesis of insulin resistance. *Physiol. Rev.*, **87**, 507–520.
28. Worley, J.R., Baugh, M.D., Hughes, D.A., Edwards, D.R., Hogan, A., Sampson, M.J. and Gavrilovic, J. (2003) Metalloproteinase expression in PMA-stimulated THP-1 cells. Effects of peroxisome proliferator-activated receptor-gamma (PPAR gamma) agonists and 9-cis-retinoic acid. *J. Biol. Chem.*, **278**, 51340–51346.
29. Yang, B., Brown, K.K., Chen, L., Carrick, K.M., Clifton, L.G., McNulty, J.A., Winegar, D.A., Strum, J.C., Stimpson, S.A. and Pahel, G.L. (2004) Serum adiponectin as a biomarker for in vivo PPARgamma activation and PPARgamma agonist-induced efficacy on insulin sensitization/lipid lowering in rats. *BMC Pharmacol.*, **4**, 4–23.
30. Kanatani, Y., Usui, I., Ishizuka, K., Bukhari, A., Fujisaka, S., Urakaze, M., Haruta, T., Kishimoto, T., Naka, T. and Kobayashi, M. (2007) Effects of pioglitazone on suppressor of cytokine signaling 3 expression: potential mechanisms for its effects on insulin sensitivity and adiponectin expression. *Diabetes*, **56**, 795–803.
31. Shan, Y., Napoli, E. and Cortopassi, G. (2007) Mitochondrial frataxin interacts with ISD11 of the NFS1/ISCU complex and multiple mitochondrial chaperones. *Hum. Mol. Genet.*, **16**, 929–941.
32. Khan, R.J., Andermann, E. and Fantus, I.G. (1986) Glucose intolerance in Friedreich's ataxia: association with insulin resistance and decreased insulin binding. *Metabolism.*, **35**, 1017–1023.

33. Rai, M., Soragni, E., Jenssen, K., Burnett, R., Herman, D., Coppola, G., Geschwind, D.H., Gottesfeld, J.M. and Pandolfo, M. (2008) HDAC inhibitors correct frataxin deficiency in a Friedreich ataxia mouse model. *PLoS ONE*, **3**, e1958.

34. Liang, H. and Ward, W.F. (2006) PGC-1{alpha}: a key regulator of energy metabolism. *Adv. Physiol. Educ.*, **30**, 145–151.

35. Davies, S.S., Pontsler, A.V., Marathe, G.K., Harrison, K.A., Murphy, R.C., Hinshaw, J.C., Prestwich, G.D., Hilaire, A.S., Prescott, S.M., Zimmerman, G.A. *et al.* (2001) Oxidized alkyl phospholipids are specific, high affinity peroxisome proliferator-activated receptor gamma ligands and agonists. *J. Biol. Chem.*, **276**, 16015–16023.

36. Marmolino, D., Acquaviva, F., Pinelli, M., Monticelli, A., Castaldo, I., Filla, A. and Cocozza, S. (2008) PPAR-gamma agonist azelaoyl PAF increases frataxin protein and mRNA expression. New implications for the Friedreich's ataxia therapy. *Cerebellum*. January 23 [Epub ahead of print], PMID: 19165552.

37. Handschin, C. and Spiegelman, B.M. (2006) Peroxisome proliferator-activated receptor gamma coactivator 1 coactivators, energy homeostasis, and metabolism. *Endocr. Rev.*, **27**, 728–735.

38. Mootha, V.K., Lindgren, C.M., Eriksson, K.F., Subramanian, A., Sihag, S., Lehar, J., Puigserver, P., Carlsson, E., Ridderstråle, M., Laurila, E. *et al.* (2003) PGC-1alpha-responsive genes involved in oxidative phosphorylation are coordinately downregulated in human diabetes. *Nat. Genet.*, **34**, 267–273.

39. Patti, M.E., Butte, A.J., Crunkhorn, S., Cusi, K., Berria, R., Kashyap, S., Miyazaki, Y., Kohane, I., Costello, M., Saccone, R. *et al.* (2003) Coordinated reduction of genes of oxidative metabolism in humans with insulin resistance and diabetes: Potential role of PGC1 and NRF1. *Proc. Natl Acad. Sci. USA*, **100**, 8466–8471.

40. Petersen, K.F., Dufour, S., Befroy, D., Garcia, R. and Shulman, G.I. (2004) Impaired mitochondrial activity in the insulin-resistant offspring of patients with type 2 diabetes. *N. Engl. J. Med.*, **350**, 664–671.

41. Nyholm, B., Qu, Z., Kaal, A., Pedersen, S.B., Gravholt, C.H., Andersen, J.L., Saltin, B. and Schmitz, O. (1997) Evidence of an increased number of type IIb muscle fibers in insulin-resistant first-degree relatives of patients with NIDDM. *Diabetes*, **46**, 1822–1828.

42. Fantus, I.G., Janjua, N., Senni, H. and Andermann, E. (1991) Glucose intolerance in first-degree relatives of patients with Friedreich's ataxia is associated with insulin resistance: evidence for a closely linked inherited trait. *Metabolism.*, **40**, 788–793.

43. Tolis, G., Mehta, A., Andermann, E., Harvey, C. and Barbeau, A. (1980) Friedreich's ataxia and oral glucose tolerance: I. The effect of ingested glucose on serum glucose and insulin values in homozygotes, obligate heterozygotes and potential carriers of the Friedreich's ataxia gene. *Can. J. Neurol. Sci.*, **7**, 397–400.

44. Schoenle, E.J., Boltshauser, E.J., Baekkeskov, S., Landin Olsson, M., Torresani, T. and von Felten, A. (1989) Preclinical and manifest diabetes mellitus in young patients with Friedreich's ataxia: no evidence of immune process behind the islet cell destruction. *Diabetologia*, **32**, 378–381.

45. Silva, J.P., Köhler, M., Graff, C., Oldfors, A., Magnuson, M.A., Berggren, P.O. and Larsson, N.G. (2000) Impaired insulin secretion and beta-cell loss in tissue-specific knockout mice with mitochondrial diabetes. *Nat. Genet.*, **26**, 336–340.

46. Ristow, M. (2004) Neurodegenerative disorders associated with diabetes mellitus. *J. Mol. Med. (Berlin, Germany)*, **82**, 510–529.

47. Lowell, B. and Shulman, G. (2005) Mitochondrial dysfunction and type 2 diabetes. *Science*, **307**, 384–387.

48. Kelley, D.E., He, J., Menshikova, E.V. and Ritov, V.B. (2002) Dysfunction of mitochondria in human skeletal muscle in type 2 diabetes. *Diabetes*, **51**, 2944–2950.

49. Duncan, J.G., Fong, J.L., Medeiros, D.M., Finck, B.N. and Kelly, D.P. (2007) Insulin-resistant heart exhibits a mitochondrial biogenic response driven by the peroxisome proliferator-activated receptor-alpha/PGC-1alpha gene regulatory pathway. *Circulation*, **115**, 909–917.

50. Finck, B.N., Lehman, J.J., Leone, T.C., Welch, M.J., Bennett, M.J., Kovacs, A., Han, X., Gross, R.W., Kozak, R., Lopaschuk, G.D. *et al.* (2002) The cardiac phenotype induced by PPARalpha overexpression mimics that caused by diabetes mellitus. *J. Clin. Invest.*, **109**, 121–130.

51. Lehman, J.J., Barger, P.M., Kovacs, A., Saffitz, J.E., Medeiros, D.M. and Kelly, D.P. (2000) Peroxisome proliferator-activated receptor gamma coactivator-1 promotes cardiac mitochondrial biogenesis. *J. Clin. Invest.*, **106**, 847–856.

52. Russell, L.K., Mansfield, C.M., Lehman, J.J., Kovacs, A., Courtois, M., Saffitz, J.E., Medeiros, D.M., Valencik, M.L., McDonald, J.A. and Kelly, D.P. (2004) Cardiac-specific induction of the transcriptional coactivator peroxisome proliferator-activated receptor gamma coactivator-1alpha promotes mitochondrial biogenesis and reversible cardiomyopathy in a developmental stage-dependent manner. *Circ. Res.*, **94**, 525–533.

53. Leone, T.C., Lehman, J.J., Finck, B.N., Schaeffer, P.J., Wende, A.R., Boudina, S., Courtois, M., Wozniak, D.F., Sambandam, N., Bernal-Mizrachi, C. *et al.* (2005) PGC-1alpha deficiency causes multi-system energy metabolic derangements: muscle dysfunction, abnormal weight control and hepatic steatosis. *PLoS Biol.*, **3**, e101.

54. Lin, J., Wu, P.H., Tarr, P.T., Lindenberg, K.S., St-Pierre, J., Zhang, C.Y., Mootha, V.K., Jäger, S., Vianna, C.R., Reznick, R.M. *et al.* (2004) Defects in adaptive energy metabolism with CNS-linked hyperactivity in PGC-1alpha null mice. *Cell*, **119**, 121–135.

55. Lin, J., Handschin, C. and Spiegelman, B.M. (2005) Metabolic control through the PGC-1 family of transcription coactivators. *Cell. Metab.*, **1**, 361–370.

56. O'Hagan, K.A., Cocchiglia, S., Zhdanov, A.V., Tambawala, M.M., Cummins, E.P., Monfared, M., Agbor, T.A., Garvey, J.F., Papkovsky, D.B., Taylor, C.T. *et al.* (2009) PGC-1{alpha} is coupled to HIF-1{alpha}-dependent gene expression by increasing mitochondrial oxygen consumption in skeletal muscle cells. *Proc. Natl Acad. Sci. USA*, **106**, 2188–2193.

57. Lynch, D.R., Farmer, J.M., Tsou, A.Y., Perlman, S., Subramony, S.H., Gomez, C.M., Ashizawa, T., Wilmot, G.R., Wilson, R.B. and Balcer, L.J. (2006) Measuring Friedreich ataxia: complementary features of examination and performance measures. *Neurology*, **66**, 1711–1716.

58. Cnop, M., Vidal, J., Hull, R.L., Utzschneider, K.M., Carr, D.B., Schraw, T., Scherer, P.E., Boyko, E.J., Fujimoto, W.Y. and Kahn, S.E. (2007) Progressive loss of beta-cell function leads to worsening glucose tolerance in first-degree relatives of subjects with type 2 diabetes. *Diabetes Care*, **30**, 677–682.

59. Kahn, S.E., Prigeon, R.L., McCulloch, D.K., Boyko, E.J., Bergman, R.N., Schwartz, M.W., Neifing, J.L., Ward, W.K., Beard, J.C., Palmer, J.P. *et al.* (1993) Quantification of the relationship between insulin sensitivity and beta-cell function in human subjects. Evidence for a hyperbolic function. *Diabetes*, **42**, 1663–1672.